Research Article Vol. 3, No. 4 / 15 April 2020 / OSA Continuum 698

OSA CONTINUUM

# Sectioning with edge extraction in optical incoherent imaging processing

YAPING ZHANG,[1,3,4] RENDE WANG,[1,5] PETER TSANG,[2] AND TING-CHUNG POON[3]

[1] *Key Lab of Laser Information Processing Technology and Application, Kunming University of Science and Technology, Kunming 650500, China*
[2] *Dept. of Electronic Engineering, City University of Hong Kong, 83 Tat Chee Avenue, Kowloon, Hong Kong SAR, China*
[3] *Bradley Dept. of Electrical & Computer Engineering, Virginia Tech, Blacksburg, Virginia 24061, USA*
[4] *yaping.zhang@gmail.com*
[5] *615987864@qq.com*

**Abstract:** Employing a single-pixel digital holographic recording technique called optical scanning holography (OSH), we accomplish the formidable task of sectioning with edge extraction in three-dimensional (3D) optical incoherent imaging. OSH is a special variant of generalized two-pupil heterodyning image processing, where one of the pupils used is a delta function with the other being a uniform function. In this study, we investigate the use of an annular pupil and a random-phase pupil for edge extraction during sectioning of a 3-D object. Novel simulation results indicate excellent edge extraction of a multi-section object with good sectioning capability, i.e., with each focused edge-extracted section out-of-focused haze has been eliminated.



## 1. Introduction

Performing image processing in incoherent optical systems is formidable. The reason is that the optical transfer function (OTF) is the autocorrelation of the pupil function of the optical system, giving in general lowpass filtering characteristics. In order to perform feature enhancement such as edge detection in optical incoherent imaging systems, two-pupil synthesis of OTFs have been explored [1–6]. In the present study, we investigate the use of optical scanning holography (OSH) for sectioning along with edge extraction in optical incoherent image processing. Optical scanning holography (OSH), operating in the incoherent mode as incoherent holography [7–9], was first implicated by Poon and Korpel [3]. It has numerous applications, including digital holographic microscopy [10,11], 3D image recognition [12], holographic image encoding and encryption [13,14], etc. The OSH system uses two-pupil optical heterodyne scanning image processing and is a single-pixel real-time digital holographic recording technology. The 3D object is raster-scanned by a structured-beam formed by the two pupils of the optical system [15]. The scattered light energy from the 3D object is collected by a single-pixel photodetector, and then the signal from the photodetector is processed by a lock-in amplifier to give two real holograms as final outputs of the optical system. Finally, a complex hologram can be formed by the two stored real holograms, which can be reconstructed numerically [16]. Reconstruction of 3D objects can be considered as a collection of two-dimensional (2D) thin sections. The reconstructed image of a hologram can be viewed visually via a spatial light modulator, or analyzed to deduce its content (a task that is commonly referred to as image analysis or object recognition). In a lot of image analysis techniques edges, instead of an image in its original form, are used in the analysis. The reason is that edges generally carry distinct information about the object shape, whereas the shaded regions bounded by the edges could be easily affected by environmental factors (such as lighting). To analyze the images represented in a hologram, it is desirable to

#383473 https://doi.org/10.1364/OSAC.383473
Journal © 2020 Received 15 Nov 2019; revised 6 Mar 2020; accepted 6 Mar 2020; published 17 Mar 2020

Corrected: 20 March 2020

OSA CONTINUUM

reconstruct the edge image directly. When focused on a particular image section of a 3D object, any defocused sections located above and below the section will also contribute to the focused plane, leading to out-of-focus haze on the image section. The blurred content in the reconstructed image degrades the edge information, leading to errors in the image analysis process that follows. Eliminating out-of-focus haze has been an important topic in the context of sectioning in digital holography. Kim has proposed to reconstruct sectional images using Wiener filtering in the context of optical scanning holography [17]. Kim et al. has investigated the relationship between fractional Fourier transform and Wigner distribution function to distinguish the information of sectional images [18]. Zhang et al. [19] and Lam et al. [20] have employed the $l_2$ norm for the first time to formulate holographic image reconstruction for sectioning. Since it is possible to use other norms, such as the $l_1$ norm, their works are considered to be the precursor to compressive holography [21]. There are other solutions such as blind sectional image reconstruction [22,23]. Edge extraction has been realized in OSH using different pupils in the optical setup such as the use of a Gaussian-ring pupil, quarter-plane pupil, spiral-phase pupil and most recently an annular pupil [24–31]. On the other hand, sectioning in OSH has also been investigated using a random-phase pupil [32–33].

In incoherent holography, sectioning has been investigated and edge extraction also has been achieved. However, sectioning and edge extraction have been considered separately until now. In our present paper, we are investigating sectioning and edge extraction to achieve edge extracted sectioning in incoherent holography. To the best of our knowledge, there are no other methods for a system with conventional pupils that generate similar results as what presents in the present paper, i.e., edge extracted sectioning. Currently there are only two incoherent digital holographic techniques: optical scanning holography (OSH), the technique being used to investigate edge extracted sectioning, and Fresnel incoherent correlation holography (FINCH) [ See reference 35 for a review ]. Edge extraction has been investigated in both of the incoherent holographic techniques, but only OSH has been investigated for sectioning of 3D objects, i.e., rejecting the out-of-focus haze on a focused section.

In this paper, a novel method to implement edge extraction of 3D objects and suppression of defocused noise during sectioning in optical incoherent imaging is proposed using OSH. An annular pupil is used as one of the pupils in OSH to extract the edge of 3D objects with the other pupil being a random-phase function to eliminate the defocused noise. In Section 2, we briefly summarize the basic principle of OSH. In Section 3, we present the complex hologram of a multi-section object and show its reconstruction, illustrating the problem of out-of-focus haze during sectioning. In Section 4, we formulate pre-processing in OSH through the use of one of the pupils in the system and explicitly we use an annular aperture for edge extraction to illustrate out-of-focus haze still existing for edge extracted sections. In Section 5, we show clear sectioning of an edge extracted section with annular and random phase pupils. Finally, in Section 6, we make some concluding remarks.

## 2. Optical scanning holography

A typical two-pupil optical heterodyne scanning system is shown in Fig. 1. $p_1(x, y)$ and $p_2(x, y)$, located on the front focal plane of lens $L_1$ of focal length $f$, are the two pupils in the system. The two pupils are illuminated by laser of frequencies $\omega_0$ and $\omega_0 + \Omega$, respectively. The upshifting of the laser frequency from $\omega_0$ to $\omega_0 + \Omega$ is accomplished conveniently by using an acousto-optic frequency shifter (AOFS) operating at frequency $\Omega$ [34]. The two optical beams from the two pupils are combined by beamsplitter $BS_2$ and then projected onto the 3-D object, which is on an x-y scanning stage.

After the 2-D scan of the object of complex amplitude $O(x, y; z)$, all the transmitted light fields (assuming the object is transmissive for simplicity here) are collected by lens $L_2$ and focused onto a single-pixel integrating photo-detector PD [35], which gives the heterodyne scanned signal at

Corrected: 20 March 2020

OSA CONTINUUM

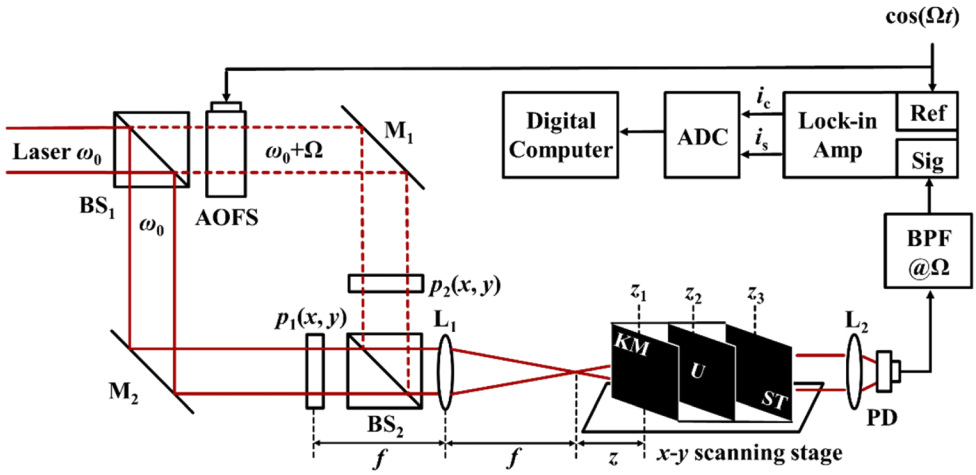


**Fig. 1.** Typical setup of two-pupil optical heterodyne scanning system. Adapted from Wang et al., "Edge extraction of multi-section objects in optical scanning holography," 28th IEEE International Symposium on Industrial Electronics, paper VD-005576, (2019). The present paper includes an extended, detailed version of this referred conference paper.

frequency Ω. The heterodyne signal is electronically filtered by a bandpass filter (BPF) centered at heterodyne frequency Ω to give the signal to the "Sig" input of the lock-in amplifier, where reference signal $\cos \Omega t$ is inputted to the "Ref" input of the lock-in amplifier. Finally the lock-in amplifier gives the in-phase and quadrature analog outputs, $i_c(x, y)$ and $i_s(x, y)$, respectively. The analog-to-digital converter (ADC) gives the digital signals to a digital computer, which finally performs a complex addition to give a complex record [15]:

$$\begin{aligned} H_c(x, y) &= i_c(x, y) + j i_s(x, y) \\ &= \int \mathfrak{I}^{-1}\{\mathfrak{I}\{|O(x, y; z)|^2\} OTF(k_x, k_y; z)\} dz, \end{aligned} \tag{1}$$

where $\mathfrak{I}$ and $\mathfrak{I}^{-1}$ denote the 2-D Fourier and inverse Fourier transforms, respectively. Again, $O(x, y; z)$ denotes a complex amplitude of the 3D object. In Eq. (1), we can see that that only the intensity distribution of the object, i.e., $|O(x, y; z)|^2$, is recorded and hence the optical system is incoherent [1–9]. Finally, $OTF$ is the optical transfer function of the system given by [6]

$$\begin{aligned} OTF(k_x, k_y; z) &= \exp[jz(k_x^2 + k_y^2)/2k_0] \\ &\times \iint p_1^*(x', y') p_2\left(x' + \tfrac{f}{k_0} k_x, y' + \tfrac{f}{k_0} k_y\right) \exp\left[j \tfrac{z}{f}(x' k_x + y' k_y)\right] dx' dy', \end{aligned} \tag{2}$$

where $k_x$ and $k_y$ denote the spatial frequencies along the $x$ and $y$ directions, respectively, $k_0 = 2\pi/\lambda$ is the wave number of the laser, and z is a depth parameter as illustrated in Fig. 1.

For purely holographic recording leading to what is commonly known as optical scanning holography (OSH) [10], we choose $p_1(x, y) = 1$, $p_2(x, y) = \delta(x, y)$, for the two-pupil system. With these chosen pupils, according to Eq. (2), we have the following holographic recording $OTF$ for optical scanning holography (OSH):

$$OTF_{OSH}(k_x, k_y; z) = \exp[-jz(k_x^2 + k_y^2)/2k_0]. \tag{3}$$

We want to point out that using a delta and uniform functions as the two pupils seem too idealistic, but they offer clarity on the idea we want to investigate. For realistic pupil functions, a narrow

OSA CONTINUUM

Gaussian function could be used instead of a delta function, and a board Gaussian function or a circular function can replace the uniform pupil function. However, we do not want to obscure the novel idea with complicated mathematical results at this stage. Nevertheless, realistic pupil functions are needed to guide us to construct any optical systems for practical applications in the next stage.

For brevity, let us assume planar object with intensity distribution $I(x, y)$ located $z_0$ away from the focal plane of lens $L_1$, i.e., $|O(x, y; z)|^2 = I(x, y)\delta(z - z_0)$. Equation (1) becomes, after integration along z,

$$\begin{aligned} H_c(x, y) &= \Im^{-1}\{\Im\{I(x, y)\}OTF_{OSH}(k_x, k_y; z_0)\} \\ &= \Im^{-1}\{\Im\{I(x, y)\}\exp[-jz_0(k_x^2 + k_y^2)/2k_0]\}. \end{aligned} \tag{4}$$

This complex record has become a complex hologram of $I(x, y)$ located $z_0$ away from the focal plane of lens $L_1$. To reconstruct the hologram, we simply need to perform Fresnel diffraction at a specific distance as follows [16]:

$$\begin{aligned} &H_c(x, y) * h(x, y; z) \\ &= \iint H_c(x', y')h(x - x', y - y'; z)\mathrm{d}x'\mathrm{d}y', \end{aligned} \tag{5}$$

where $*$ denotes 2D convolution, and $h(x, y; z) = \exp(-jk_0 z)\frac{jk_0}{2\pi z}\exp[-jk_0(x^2 + y^2)/2z]$ is the spatial impulse response in Fourier optics [16].

## 3. Out-of-focus haze upon conventional sectioning

Let us consider a 3-section object with the sections perpendicular to the scanning beam and having the spatial distance at locations $z_1$, $z_2$, and $z_3$, as shown in Fig. 1. The complex hologram of the multi-section object, according to Eq. (1) but in a discrete form, is given by

$$H_c(x, y) = \sum_{i=1}^{3} \Im^{-1}\{\Im\{|O(x, y; z_i)|^2\}OTF_{OSH}(k_x, k_y; z_i)\}. \tag{6}$$

For standard OSH and the three-section object shown in Fig. 2(a), Fig. 2(b) and 2(c) are the in-phase and quadrature outputs, $i_c(x, y)$ and $i_s(x, y)$, of the 3D object, respectively. The in-phase and quadrature outputs are also commonly known as the cosine and sine holograms, respectively [15]. The parameters used in the simulation are as follows. The wavelength $\lambda$ of the laser is 632 nm. The multi-section object is a transparent image of 512 × 512 pixels with the size of

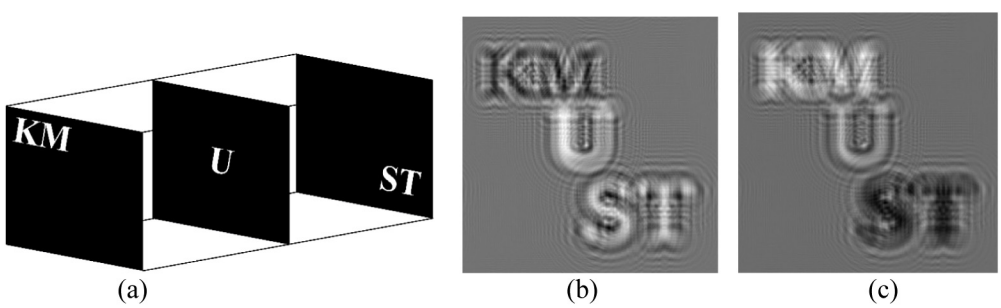


**Fig. 2.** (a) Original 3-section object, (b) and (c) In-phase and quadrature outputs (cosine and sine holograms, respectively) of the 3-section object.

Corrected: 20 March 2020

OSA CONTINUUM

2 cm × 2 cm. The focal length $f$ of lens $L_1$ is 200 mm. The distance parameters of $z_1$, $z_2$ and $z_3$, are 14 mm, 16 mm and 18 mm, respectively. Figure 3 shows the reconstruction of the complex hologram at perspective locations of the 3-section object. In Fig. 3(a), "KM" is focused with the other two sections out-of-focused. The out-of-focus section information on the focused section is considered to be the out-of-focus haze contributing to the focused section. Similarly, Figs. 3(b) and 3(c) show the sharp sections corresponding to "U" and "ST", respectively with out-of-focus haze from other sections.


(a) (b) (c)

**Fig. 3.** Reconstructed images of three sections, illustrating out-of-focus haze on the focused sections.

## 4. Pre-processing

### 4.1. With annular pupil

For the two-pupil system shown in Fig. 1, we now choose $p_2(x, y) = \delta(x, y)$ but with $p_1(x, y) = a(r; \varepsilon, w_2) = circ(r/w_2) - circ(r/w_1)$, where $r = \sqrt{x^2 + y^2}$ and $circ(r/r_0)$ denotes a value 1 within a circle of radius $r_0$ and 0 otherwise. $w_2$ and $w_1$ are outer and inner radii of annulus $a(r; \varepsilon, w_2)$, respectively, with a central obscuration ratio of the annulus defined by $\varepsilon = w_1/w_2$. For the above two pupils, the OTF in Eq. (2) becomes

$$\begin{aligned} OTF_{ANN}(k_x, k_y; z) &= \exp\left[\frac{-jz(k_x^2+k_y^2)}{2k_0}\right][circ(\tfrac{k_r}{r_2}) - circ(\tfrac{k_r}{r_1})] \\ &= \exp\left[\frac{-jz(k_x^2+k_y^2)}{2k_0}\right] a(k_r; \varepsilon, r_2), \end{aligned} \tag{7}$$

where $k_r = \sqrt{k_x^2 + k_y^2}$, $r_2 = w_2 k_0/f$, $r_1 = w_1 k_0/f$ and $\varepsilon = r_1/r_2 = w_1/w_2$ . Note that the magnitude of the OTF is of the same functional form of the annulus with the central obscuration ratio being the same as that in the physical annular pupil. $a(k_r; \varepsilon, r_2)$ in Eq. (7) is a bandpass filter. For the planar object with intensity distribution $I(x, y)$ located $z_0$ away from the focal plane of lens $L_1$ as described in the last section, the complex hologram becomes

$$\begin{aligned} H_c(x, y) &= \Im^{-1}\{\Im\{I(x, y)\} a(k_r; \varepsilon, r_2) \exp[-jz_0(k_x^2 + k_y^2)/2k_0]\} \\ &= \Im^{-1}\{\Im\{I(x, y)\} a(k_r; \varepsilon, r_2) OTF_{OSH}(k_x, k_y; z_0)\}. \end{aligned} \tag{8}$$

Note that from the above we can see that the spectrum of the object, i.e., $\Im\{I(x, y)\}$, is first bandpass filtered by annular filter $a(k_r; \varepsilon, r_2)$ before holographic recording. Hence, it performs preprocessing of holographic information. Indeed, pre-processing of holographic information in film-based systems has been difficult to implement, albeit important so as to improve the

OSA CONTINUUM

fringe contrast before holographic recording [36,37]. Schilling and Poon was the first to propose real-time pre-processing in optical scanning holography [24]. In their simulations of the idea of pre-processing of holographic information, they have used a Gaussian-ring function for $p_1(x, y)$ to extract the edge information of an object. We have used an annulus of $\varepsilon = 0.5$ in our simulations and it is shown in Fig. 4(a) along with the spectrum of one sectional image, "KM", shown in Fig. 4(b) as a comparison on the relative sizes of the spectrum and annular filter $a(k_r; \varepsilon, r_2)$.

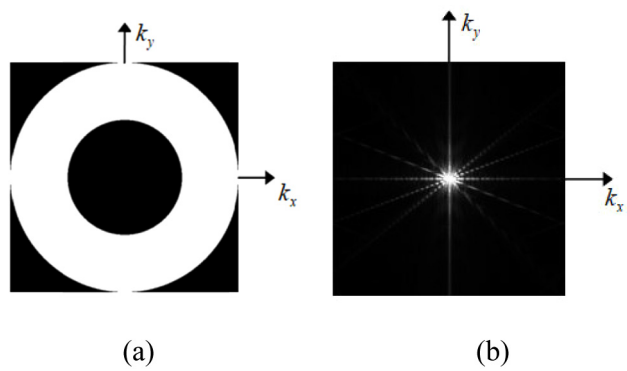


**Fig. 4.** (a) Annular filter $a(k_r; \varepsilon, r_2)$ of $\varepsilon = 0.5$;(b) Intensity spectrum of the "KM" section.

Figure 5(a) and (b) are the in-phase and quadrature holograms of the 3D object being processed by the OTF given by Eq. (7). Figure 6(a), 6(b) and 6(c) show the reconstructed images of the three sections of the multi-section image. Clearly, the use of an annular pupil is capable of extracting edges for the 3-D object. However, we still notice the out-of-focus haze for each focused section.

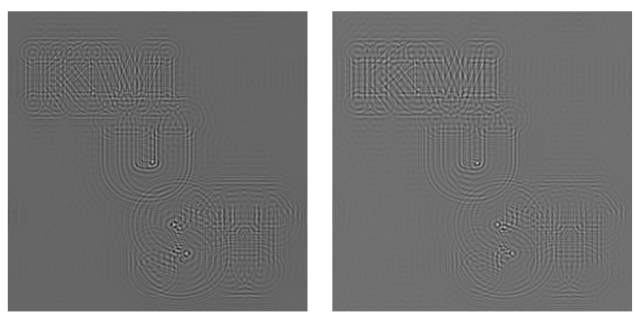


**Fig. 5.** (a) and (b) In-phase and quadrature holograms with annular pupil, respectively.

### 4.2. *With random phase pupil*

For $p_1(x, y) = 1$ and $p_2(x, y) = \exp[j2\pi s(x, y)]$. where $s(x, y)$ denotes an independent random function uniformly distributed in the interval [0-1], the OTF according to Eq. (2) becomes

$$\begin{aligned} OTF_{RP}(k_x, k_y; z) &= \exp[jz(k_x^2 + k_y^2)/2k_0] \\ &\times \iint \exp\left[j2\pi s\left(x' + \tfrac{f}{k_0}k_x, y' + \tfrac{f}{k_0}k_y\right)\right] \exp\left[j\tfrac{z}{f}(x'k_x + y'k_y)\right] dx'dy'. \end{aligned} \tag{9}$$

OSA CONTINUUM


(a) (b) (c)

**Fig. 6.** Reconstructed images of three sections with annular pupil. Note the out-of-focus haze on the focused plane.

The complex hologram in this case, according to Eq. (6), is

$$H_c(x, y) = \sum_{i=1}^{3} \mathfrak{I}^{-1}\{\mathfrak{I}\{|O(x, y; z_i)|^2\} OTF_{\mathrm{RP}}(k_x, k_y; z_i)\}. \tag{10}$$

Figure 7 shows the in-phase and quadrature holograms of the situation and Fig. 8 shows the

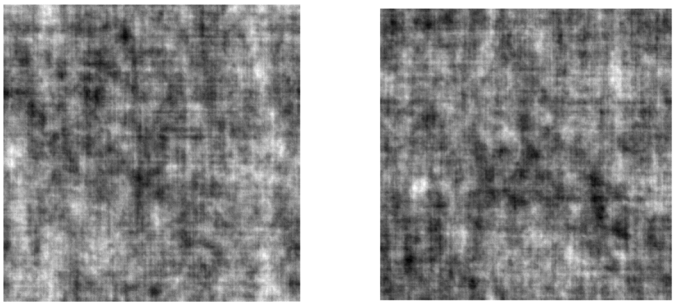

(a) (b)

**Fig. 7.** a) and b) In-phase and quadrature holograms with random phase as one of the pupils and the other pupil being uniform.

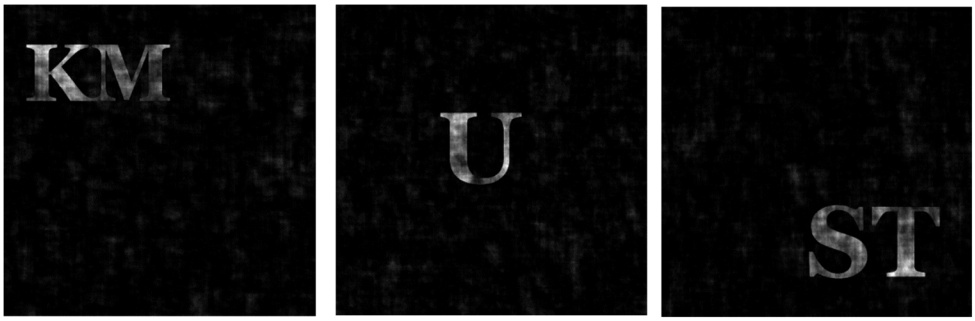


(c) (d) (e)

**Fig. 8.** Reconstructed images of three sections with random phase pupil.

Corrected: 20 March 2020

OSA CONTINUUM

reconstruction for the three sections. Note that there is essentially no out-of-focus haze on each edge extracted section. However, there are some speckle-like noise superimposed on the reconstructed images due to the use of a random phase pupil.

## 5. Sectioning with annular and random phase pupils

As pointed out from the last section that edge extraction has been performed successfully by using an annular pupil, however, the out-of-focus haze issue remains. In this section, we propose the use of annular and random phase pupils for sectioning edge extracted sections to get rid of the haze. We let $p_1(x, y) = a(r; \varepsilon, w_2)$ and $p_2(x, y) = \exp[j2\pi s(x, y)]$, The OTF, according to Eq. (2), becomes

$$\begin{aligned} OTF_{\text{sec}}(k_x, k_y; z) &= \exp[jz(k_x^2 + k_y^2)/2k_0] \\ &\times \iint a(r'; \varepsilon, w_2) \exp\left[j2\pi s\left(x' + \tfrac{f}{k_0}k_x, y' + \tfrac{f}{k_0}k_y\right)\right] \exp\left[j\tfrac{z}{f}(x'k_x + y'k_y)\right] dx'dy', \end{aligned} \tag{11}$$

where $r' = \sqrt{(x')^2 + (y')^2}$. For this OTF and according to Eq. (6), the complex hologram becomes

$$H_c(x, y) = \sum_{i=1}^{3} \mathfrak{I}^{-1}\{\mathfrak{I}\{|O(x, y; z_i)|^2\} OTF_{\text{sec}}(k_x, k_y; z_i)\}. \tag{12}$$

Figure 9 shows the in-phase and quadrature holograms of the situation and Fig. 10 shows the reconstruction for the three sections. Note that there is essentially no out-of-focus haze on each edge extracted section.

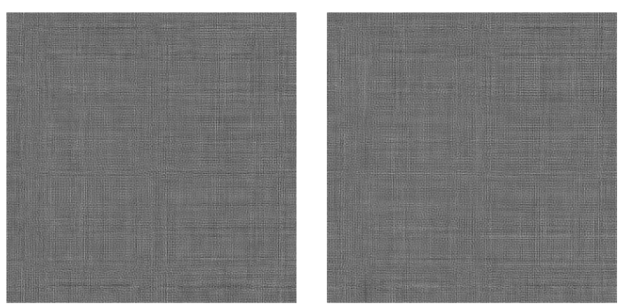

(a) (b)

**Fig. 9.** a) and b) In-phase and quadrature holograms with random phase as one of the pupils and the other pupil being the same annular pupil as in Section 4.

While we have seen effective edge extraction using annular pupil, detail of the edge has not been fully explored. We have seen that the use of annular pupil in the two-pupil system corresponds to bandpass filtering in incoherent optical systems. In any case, in coherent image processing systems, the use of an annular pupil has led to zero-detection of the edge [38], effectively corresponding to a second-order differentiation operation. Indeed the same result applies to the optical incoherent two-pupil system under consideration, where the simulated hologram actually contains the edge information only. Figure 11(a) shows an enlarged image of Fig. 10(b) and Fig. 11(c) is the intensity of the red line trace across the reconstructed image from Fig. 11(a). Obviously, we see a zero-detection of the edge. We also observe some noise in the output, which is due to the use of a random phase pupil as shown in Fig. 8 on the focused reconstruction plane. Accordingly, a simple post-processing threshold method has been used

OSA CONTINUUM

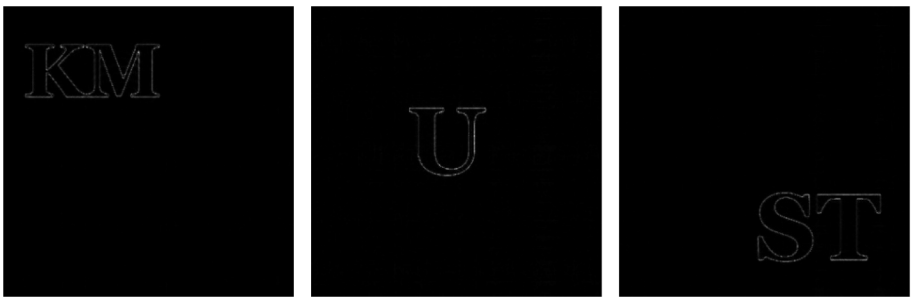


(a) (b) (c)

**Fig. 10.** Sectional reconstructed images of three sections. Note that there are no out-of-focus haze on the focused plane.

to improve the signal-to-nose ratio in the final image reconstruction. The adaptive threshold method basically calculates a threshold according to the neighborhood of the image pixel, and compares the value of each pixel with the average of the neighboring pixels. If the value of a pixel differs greatly from its local average, it is taken to be high. Otherwise, it is taken to be low. Figures 11(b) and 11(d) show the adaptive versions of Fig. 11(a) and 11(c), respectively.

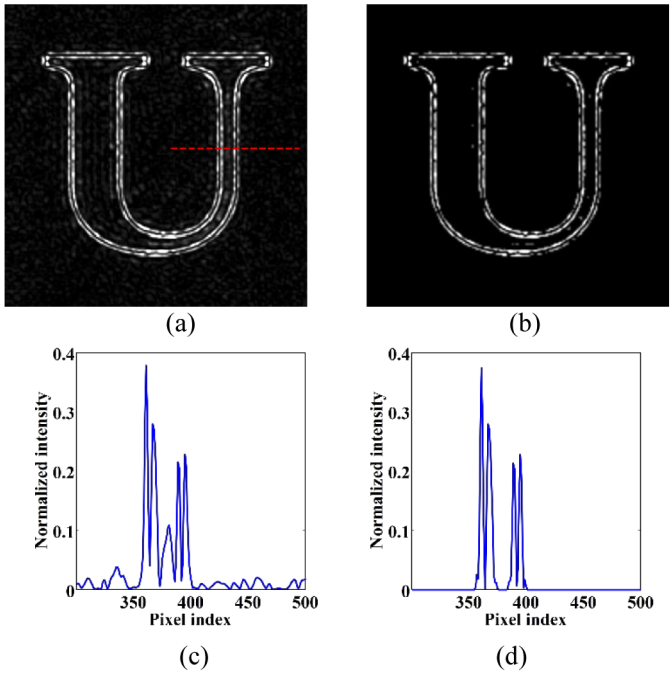


**Fig. 11.** (a) Magnified version of "U" from Fig. 10(b). (b) Output of Fig. 11(a) processed by a simple adaptive threshold method. (11c) and (11d) show the line trace across the portion of the reconstructed images of Figs. 11(a) and 11(b), respectively.

## 6. Concluding remarks

We have shown that by manipulating of the pupils in optical scanning holography, we have achieved edge-extracted sectioning in optical scanning holography. The process is akin to

OSA CONTINUUM

pre-processing of digital holographic information. Explicitly, we have investigated the use of an annular pupil and a random phase pupil in optical scanning holography for a multi-section edge extraction plus sectioning without out-of-focus haze. We have found excellent edge extraction capabilities with the annular pupil alone for a 3-D object but with out-of-focus haze. In other words, clear sectioning capability is low. However, with both the annular and random phase pupils, the system performs excellent edge-extracted sectioning. Current simulations employ an annulus with a single value of the central obscuration ratio. It is instructive to see the performance of edge extraction as a function of the obscuration ratio as well as the center frequency of the passband. We plan to investigate these aspects in the near future.

## Funding

National Natural Science Foundation of China (11762009, 61565010, 61865007); Natural Science Foundation of Yunnan Province (2018FB101); the Key Program of Science and Technology of Yunnan Province (2019FA025); the General Research Fund (GRF) of Hong Kong SAR (9042822).

## Disclosures

The authors declare no conflicts of interest.

## References

1. W. Lohmann and W. T. Rhodes, "Two-pupil synthesis of optical transfer functions," Appl. Opt. **17**(7), 1141–1150 (1978).
2. W. Stoner, "Incoherent optical processing via spatially offset pupil masks," Appl. Opt. **17**(15), 2454–2466 (1978).
3. T.-C. Poon and A. Korpel, "Optical transfer function of an acousto-optic heterodyning image processor," Opt. Lett. **4**(10), 317–319 (1979).
4. G. Indebetouw and T.-C. Poon, "Novel Approaches of incoherent Image Processing with Emphasis on Scanning Methods," Opt. Eng. **31**(10), 2159–2167 (1992).
5. R. A. Athale, J. van der Gracht, D. W. Prather, and J. N. Mait, "Incoherent optical image processing with acousto-optic pupil-plane filtering," Appl. Opt. **34**(2), 276–280 (1995).
6. T.-C. Poon, "Scanning holography and two-dimensional image processing by acousto-optic two-pupil synthesis," J. Opt. Soc. Am. **2**(4), 521–527 (1985).
7. T. Tsuruta, "Holography using an extended spatially incoherent source," J. Opt. Soc. Am. **60**(1), 44–48 (1970).
8. B. Breckinridge, "Two-dimensional white light coherence interferometer," Appl. Opt. **13**(12), 2760–2762 (1974).
9. O. Bryngdahl and A. Lohmann, "Variable magnification in incoherent holography," Appl. Opt. **9**(1), 231–232 (1970).
10. T.-C. Poon, K. Doh, G. Indebetouw, B. W. Schilling, M. Wu, K. Shinoda, and Y. Suzuki, "Three-dimensional microscopy by optical scanning holography," Opt. Eng. **34**(5), 1338–1344 (1995).
11. B. W. Schilling, T.-C. Poon, G. Indebetouw, B. Storrie, K. Shinoda, Y. Suzuki, and M. H. Wu, "Three-dimensional holographic fluorescence microscopy," Opt. Lett. **22**(19), 1506–1508 (1997).
12. T.-C. Poon and T. Kim, "Optical image recognition of three-dimensional objects," Appl. Opt. **38**(2), 370–381 (1999).
13. A. Yan, Y. Wei, Z. Hu, J. Zhang, P. W. M. Tsang, and T.-C. Poon, "Optical cryptography with biometrics for multi-depth objects," Sci. Rep. **7**(1), 12933 (2017).
14. T.-C. Poon, T. Kim, and K. Doh, "Optical scanning cryptography for secure wireless transmission," Appl. Opt. **42**(32), 6496–6503 (2003).
15. T.-C. Poon, "Optical scanning holography - a review of recent progress," J. Opt. Soc. Korea **13**(4), 406–415 (2009).
16. T.-C. Poon and J.-P. Liu, *Introduction to Modern Digital Holography with MATLAB*, Cambridge University Press (2014).
17. T. Kim, "Optical sectioning by optical scanning holography and a Wiener filter," Appl. Opt. **45**(5), 872–879 (2006).
18. H. Kim, S.-W. Min, B. Lee, and T.-C. Poon, "Optical sectioning for optical scanning holography using phase-space filtering with Wigner distribution functions," Appl. Opt. **47**(19), D164–D175 (2008).
19. X. Zhang, E. Y. Lam, and T.-C. Poon, "Reconstruction of sectional images in holography using inverse imaging," Opt. Express **16**(22), 17215–17226 (2008).
20. E. Y. Lam, X. Zhang, H. Vo, T.-C. Poon, and G. Indebetouw, "Three-dimensional microscopy and sectional image reconstruction using optical scanning holography," Appl. Opt. **48**(34), H113–H119 (2009).
21. D. J. Brady, K. Choi, D. l. L. Marks, R. Horisaki, and S. Lim, "Compressive Holography," Opt. Express **17**(15), 13040–13049 (2009).
22. P. W. M. Tsang, K. W. K. Cheng, T. Kim, Y. S. Kim, and T.-C. Poon, "Fast reconstruction of sectional images in digital holography," Opt. Lett. **36**(14), 2650–2652 (2011).

OSA CONTINUUM


23. X. Zhang, E. Y. Lam, T. Kim, Y. S. Kim, and T.-C. Poon, "Blind Sectional Image Reconstruction for Optical Scanning Holography," Opt. Lett. **34**(20), 3098–3100 (2009).
24. B. W. Schilling and T.-C. Poon, "Real-time preprocessing of holographic information," Opt. Eng. **34**(11), 3174–3180 (1995).
25. T.-C. Poon and K. B. Doh, "On the theory of optical Hilbert transform for incoherent objects," Opt. Express **15**(6), 3006–3011 (2007).
26. Y. Pan, W. Jia, J. Yu, K. Dobson, C. Zhou, Y. Wang, and T.-C. Poon, "Edge extraction using a time-varying vortex beam in incoherent digital holography," Opt. Lett. **39**(14), 4176–4179 (2014).
27. X. Zhang and E. Y. Lam, "Edge detection of three-dimensional object by manipulating pupil functions in optical scanning holography system," in *IEEE International Conference on Image Processing*, pp. 3661–3664, September 2010.
28. Y. Zhang, R. Wang, L. Wang, P. Tsang, and T.-C. Poon, "Annular pupil in optical scanning holography," in *2019 OSA Topical Meeting on Digital Holography and Three-Dimensional Imaging*, Paper W1A.5.
29. R. Wang, Y. Zhang, T.-C. Poon, and P. Tsang, "Edge extraction of multi-section objects in optical scanning holography," in *2019 The 28th IEEE International Symposium on Industrial Electronics*, paper VD-005576.
30. R. D. Wang, Y. P. Zhang, F. Wang, X. F. Zhu, C. G. Li, Y. A. Zhang, and W. Xu, "Edge extraction based on optical scanning holography system with annular pupils," Chin. J. Lasers **46**, 0109001 (2019).
31. Y. Zhang, T.-C. Poon, P. W. M. Tsang, R. Wang, and L. Wang, "Review on feature extraction for 3-D incoherent image processing using optical scanning holography," IEEE Trans. Ind. Inf. **15**(11), 6146–6154 (2019).
32. Z. Xin, K. Dobson, Y. Shinoda, and T.-C. Poon, "Sectional image reconstruction in optical scanning holography using a random-phase pupil," Opt. Lett. **35**(17), 2934–2936 (2010).
33. C.-J. Xiao, X. Zhou, J.-P. Hu, J. Xie, Y. Wang, and X. F. Guo, "A theoretical investigation into the 3D point spread situation of a scanning holographic imaging system based on random phase encoding," Opt. Laser Technol. **50**, 20–24 (2013).
34. T.-C. Poon and T. Kim, Ch. 4, *Acousto-Optics, Optical Engineering with MATLAB*, 2nd ed., World Scientific, 2018.
35. J.-P. Liu, T. Tahara, Y. Hayasaki, and T.-C. Poon, "Incoherent digital holography: a review," Appl. Sci. **8**(1), 143 (2018).
36. G. Molesini, D. Bertani, and M. Cetca, "In-line holography with interference filters as Fourier processors," Opt. Acta **29**(4), 479–484 (1982).
37. C. Ozkul, D. Allano, and M. Trinite, "Filtering effects in far-field in-line holography," Opt. Eng. **25**(10), 2830–2835 (1986).
38. X. Yang, W. Jia, D. Wu, and T.-C. Poon, "On the difference between single- and double-sided bandpass filtering of spatial frequencies," Opt. Commun. **384**, 71–77 (2017).


Corrected: 20 March 2020